Journal of Applied Physics

Pulse response of the GaAs/GaAsP superlattice photocathode

Cite as: J. Appl. Phys. **132**, 185702 (2022); https://doi.org/10.1063/5.0108675
Submitted: 09 July 2022 • Accepted: 29 September 2022 • Published Online: 08 November 2022

Nahid Scahill and Kurt Aulenbacher

Journal of Applied Physics ARTICLE scitation.org/journal/jap

Pulse response of the GaAs/GaAsP superlattice photocathode

Cite as: J. Appl. Phys. **132**, 185702 (2022); doi: 10.1063/5.0108675
Submitted: 9 July 2022 · Accepted: 29 September 2022 ·
Published Online: 8 November 2022

Nahid Scahill[a] and Kurt Aulenbacher[b]

AFFILIATIONS

Helmholtz Institute Mainz, Mainz, Germany and GSI Helmholtzzentrum for Schwerionenforschung, Darmstadt, Germany

[a]**Author to whom correspondence should be addressed:** nscahill@uni-mainz.de
[b]**Also at:** Institut für Kernphysik, Johannes Gutenberg Uniersität Mainz, Germany.

ABSTRACT

Pulse responses of different materials commonly used as electron sources in photoinjectors have been determined. Thin film photocathodes, such as strained GaAs/GaAsP superlattice and K_2CsSb, produce fast responses. The emission intensity at time scales comparable with the acceptance of electron accelerators is found to be reasonably low, which is an advantage for operation at high beam powers. The temporal responses of these cathodes are compared with the response of bulk GaAs.

I. INTRODUCTION

Photocathodes capable of delivering beams with high brightness are in use in many modern electron accelerators, in particular, as drivers for FEL (Free Electron Laser). When a spin-polarized beam is required, photocathodes based on III/V compounds with a surface activated to negative electron affinity (NEA) are state of the art. The results presented in this paper are related to the application of such beams in high average power electron accelerators used for particle physics. A current example is the P2-experiment: the investigation of the electro-weak mixing angle $\sin^2(\theta_W)$ in an experiment at the Mainz Energy-Recovering Superconducting Accelerator[1] (MESA), which is under construction at the Johannes Gutenberg University in Mainz.[2]

The time response of the cathode must be within the longitudinal acceptance of the accelerator. Accelerating particles with an RF-system needs a sharp longitudinal bunch compression at the entrance of the RF-cavities. This process is achieved by an approximately linear velocity modulation with a buncher-cavity. For a standard buncher, the linear region has an extension of approximately 60° within the RF-period, which corresponds to less than 70 ps for the (MAinzer MIkroton) MAMI-frequency of 2.449 GHz.[3] The part of the emitted electron distribution ("the bunch") that does not fulfill this condition is called "longitudinal halo." The longitudinal halo causes beam loss during the acceleration process. To characterize the problem, it is noted that power losses of the order of only a few tens of Watt can already produce serious concerns at high-energy accelerators due to the induced radioactivity. Moreover, precision experiments can be seriously hampered by backgrounds from the halo even with losses at much lower levels. In the P2-experiment at MESA, the beam power is more than 20 kW; hence, it demands the control of such losses to the level below 10^{-4}. Perhaps much stricter requirements are caused by the fact that superconducting RF-cavities can quench due to the small local heat loads (<1 W), which can be induced by much smaller relative losses. The motivation to minimize the longitudinal halo becomes much more important for future facilities such as the LHeC,[4] where beam powers in the multi-megawatt range are being discussed. The problem of the longitudinal halo can be somewhat mitigated by the use of longitudinal collimation systems at low energy, the so-called choppers. However, their operation is complicated and often cannot suppress the halo to the desirable high degree. Therefore, it is preferable to meet the accelerator requirement by producing a suitably well-defined electron bunch directly at the electron source.

In the case of the photo-emitted bunches, the energy width is small compared to the energy acceptance of the accelerator. Therefore, the challenge of matching the longitudinal acceptance is lessened to producing a suitable time response of the photocathode. Although it is seemingly easy to produce a laser pulse that matches the requirements, the actual time response of the cathode sets the

lower limit to the fraction of the response outside the accelerator acceptance. The RMS width of the emitted distribution is according to the properties of the cathode material and is relatively easy to estimate. On the contrary, the tail of the distribution may depend on the details of the cathode bulk or on the surface structure. The purpose of the present paper is to investigate the tail of the distribution for the case of the most frequently used photocathode for spin-polarized beam, namely, the NEA GaAs/GaAsP superlattice.

For the superlattice, it is expected that the mean free path of conduction band electrons is of the same order as the layer thickness (few tens of nm vs 100 nm). Our earlier experimental studies with GaAsP- and GaAs-films of similar active layer thickness[5] could not detect emission after a few picoseconds. Later, this finding was supported by a computer simulation study which used a random walk model.[6] However, at the time, the tail of the response could be investigated with an experimental sensitivity limited to a few percent relative to the maximum of the emission. On the other hand, in the investigation of the GaAlInAs/GaAlAs-type superlattice with enhanced sensitivity, the observed responses in the high intensity part of the response were repeatedly in agreement with the prediction. However, a long tail with an intensity at the 1% level was observed which was attributed to the defects in the superlattice structure.[7,8]

Positive electron affinity (PEA) cathodes, such as K_2CsSb, require electrons traveling with surplus energy over the conduction band minimum in order to overcome the energy barrier at the surface. As it is pointed out, for example, by Spicer and Herrera-Gomez,[9] the energy loss in the conduction band results in the reduction of the emission with a time constants of less than a picosecond. Therefore, no emission is expected outside of the profile of the drive-laser pulse at the picosecond level. Unfortunately, PEA cathodes do not permit achieving sufficient electron spin polarization. However, they have potential for application, e.g., for high intensity linacs, which in turn may serve as drivers for synchrotron radiation sources.[10] The results concerning the tails of the GaAs/GaAsP superlattice and a K_2CsSb sample are presented in Fig. 6. The measurements were conducted using the PKAT (Polarisierte KAnone Test) apparatus which is described in detail in earlier publications.[5,7,11] As a new ingredient, the high dynamic range offered by the PKAT is used.

II. MATERIALS AND METHODS

A. Negative electron affinity photocathodes

Negative electron affinity GaAs and GaAs-based photocathodes are presently the material of choice for producing spin-polarized beams for linear electron accelerators.[3,12–14] GaAs-based photocathodes have the ability of providing high spin polarization in strained superlattice structures, a sufficiently high quantum efficiency (QE), defined as the number of emitted electrons per incoming photons, and low emittance. For the very thin layer cathodes, the specific requirement of operating close to the bandgap reduces the achievable QE by more than an order of magnitude compared to the bulk GaAs, where very high QEs of almost 50% have frequently been reported—see, for instance, Spicer and Herrera-Gomez[9] and references therein. In the case of our superlattice, in the wavelength region used in the investigation, the active layer thickness is estimated approximately an order of magnitude smaller than the absorption length. This difference, in turn, reduces the obtained QE accordingly. In applications where spin-polarized beams are needed, attaining high polarization is essential and outweighs the low QE.

The NEA photocathodes require an ultrahigh vacuum (UHV) system with base vacuum pressure in the regime 10^{-11} mbar or lower to provide a sufficiently long lifetime. In machines where spin polarization is not of major importance, the use of the NEA cathodes is less desirable due to the complications associated with the UHV system and several other stringent requirements. For example, the beam losses in the vicinity of the cathode must be avoided in order to achieve a reasonable lifetime for the cathode. Acceptable losses must be of the order of nanoampere in order to achieve a lifetime of >1000h.[15,16] Note that this problem is not directly related to the losses in the accelerator which are caused by the longitudinal halo since beam losses in the vicinity of the cathode occur between the source and the entrance into the RF-system. On the other hand, NEA photocathodes are presently indispensable when spin-polarized beams are needed. An overview of the conditions required to operate an NEA cathode at an accelerator is given elsewhere.[16]

The state of NEA is achieved through co-deposition of Cs and O_2 layers on the highly p-doped and ultra-clean GaAs surface. This process brings the vacuum level below the conduction band minimum. This is a necessary condition to allow the electrons reach the surface and tunnel into the vacuum. The photocathode temporal response time predominantly depends on the optical penetration depth of the laser and the electron escape depth. The process of photoemission from a NEA photocathode is described with Spicer's three-step model.[9] These steps are *photoexcitation* of electrons from the valence band into the conduction band, *transport* of electrons to the surface, and *emission* of electrons from the surface into the vacuum. Whereas the first step happens on extremely short time scale, the second and the third steps may create a considerable width of the impulse response, which in turn, may lead to the creation of the longitudinal halo.

B. Strained GaAs/GaAs superlattice

The photocathode used in the experiment is a strained GaAs/GaAsP superlattice. This strained superlattice (SSL), which first was created by proper methods for optoelectronic devices and was published by Ref.17, is commercially fabricated by SVT Associates.[18] Figure 1 illustrates the structure of the strained GaAs/GaAsP superlattice which is investigated in this project.

The strained superlattice is grown by Molecular Beam Epitaxy (MBE) and consists of 14 pairs of alternating strained layers of GaAs and GaAsP in the active layer with a total thickness of ≈92 nm for the active region. The very high quality of growth was, for example, confirmed by the stepwise increase of the density of states which is typical for the 2D-structure of the SSL, see further explanation in Maruyama *et al.*[17] The quality of growth manifests itself by the corresponding stepwise increase of QE with increasing excitation energy.[17]

The heterostructure of the superlattice breaks the degeneracy of the crystal structure in the valence band. Using circularly polarized light with the proper energy allows selective excitation of electrons from one type of spin state in the valence band to another

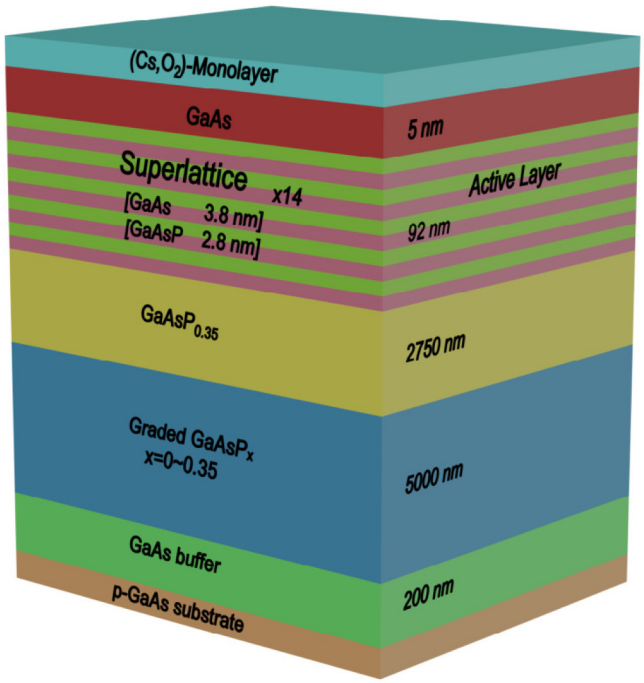

FIG. 1. Schematic crystal layer structure of strained GaAs/GaAsP superlattice which is investigated in this work.

one in the conduction band.[19] The crystal, however, provides well-defined spin states only at the band edges. This condition, in turn, requires that a cathode for spin-polarized beams to be excited with near-bandgap energy photons. This requirement, in turn, necessitates achieving the NEA surface state to make photoemission into vacuum energetically possible.

The active layer of the superlattice is very thin and, therefore, a very short response in the order of picoseconds can be expected.[5] This assumption was confirmed in an investigation of InAlGaAs/AlGaAs superlattices, but a rather high pedestal was observed after the initial steep drop in the pulse intensity.[8] This behavior was attributed to defects in the multilayer structures which were produced by Metal Organic Chemical Vapor Deposition (MOCVD). Since in our case, the GaAs/GaAsP structures are produced by MBE,[17] a technology that in principle can provide better control of the growth process, one could hope for better results here. This hypothesis was indeed confirmed, as it is shown below.

C. Experimental setup

A picture of the PKAT transport system, which consists of a 45 keV DC photoemission electron source, a beam diagnostic line, and a photocathode laser system is shown in Fig. 2. For simplicity, only the elements which are relevant for the time-resolved measurements of the intensity and polarization of the electron pulses are highlighted in color.

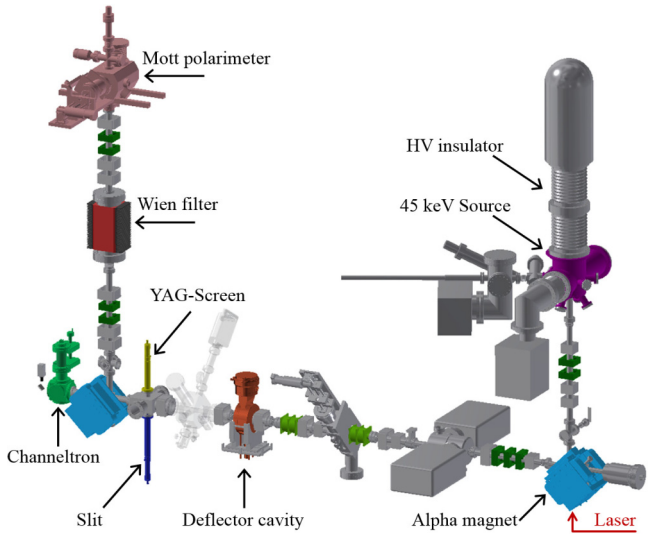

FIG. 2. Overview of the schematic structure of the PKAT transport beam line.

The femtosecond laser (shown with red arrow) illuminates the photocathode from below, and the generated electron pulses travel through the beam line. The pulses go through the deflector cavity and the slit and into the channeltron for the pulse response measurements. Alternatively, the transmitted fraction through the slit can be guided through the deflecting magnet (shown in blue) into the Wien filter spin rotator and in the Mott polarimeter for the time-resolved polarization measurements, as it is shown in Fig. 2. The latter measurements result in Mott scattering asymmetry as illustrated in Fig. 4. The details of these measurements are discussed elsewhere.[20]

The PKAT source is essentially a copy of the 100 keV source operating at MAMI,[3] which has a triode structure with an intermediate electrode operating at nominally 50 keV. Due to a defective high voltage insulator in the source chamber, the PKAT source is no longer able to reach its design energy of 100 keV. In order to avoid discharges, which cause cathode destruction, the source was operated at 45 kV. The defective lower insulator in the source chamber was removed. The intermediate electrode in the chamber was kept and grounded (0 V potential) compared to being kept at 50 kV in the original design.

This arrangement provided mitigation of the problem arising from the deviation of the design energy since the now grounded intermediate electrode surrounds the cathode electrode apart from the opening through which the beam passes. At 45 kV, the potential difference between the two metal surfaces is approximately the same as before, hence the electric field configuration in the cathode region is relatively sustained. This condition allowed maintaining two important properties. First, the missing electric field in the second stage of acceleration between the previously 50 kV electrode and the anode is of minor importance since the main focusing action is generated by the electric field in the cathode region. In consequence, the arrangement of focusing lenses in the beamline did not need to be revised. Second, the electric field strength in the cathode region could be maintained at a fairly similar field strength

to the PKAT in the original design, approximately 1 MV m^{-1} at the crystal surface. This fact helps to mitigate the transit time spread which can deteriorate the time resolution of the apparatus.[5]

D. Time response measuring principle

The principle of the temporal response measurements is shown in Fig. 3. A mode-locked Ti:Sapphire laser produces femtosecond pulses with 78.1 MHz repetition rate to illuminate the photocathode. The laser pulses are synchronized to the 32nd subharmonics of a 2.499 GHz deflecting cavity resonator frequency. In the deflector cavity, the profile of the electron bunches is transferred from longitudinal to transverse. A phase shifter induces a time delay in the electron pulses arrival at the deflector cavity, and thereby, the electrons are deflected differently in the transverse direction. At each constant phase, many individual electron pulses are integrated.

The transverse profile of the electron bunches can be analyzed either directly on a YAG screen or with a channeltron after passing through a 100 μm slit. The pulse response measurements in this project are obtained by using the latter method. The channeltron offers a high dynamic range, and, therefore, the longitudinal halo can be investigated. The channeltron can, in principle, detect single electrons. However, in our case, the channeltron was used as an analog amplifier for the average electron current behind the slit. The channeltron was operated with a moderate amplification of ≈1000 followed by a conventional ammeter. Since x-rays are not generated very effectively at our operating voltage and furthermore, there exists a strong shielding by the housing of the slit, no additional measures against parasitic x-ray were necessary. A detailed description of the experimental setup has been published by Hartmann *et al.*[11]

By keeping the slit fixed and shifting the phase between the laser and the deflector cavity in small steps, the electron arrival time at the deflector cavity is varied, and, thus, different parts of the longitudinal profile are sampled. This process allows scanning the complete profile of the electron pulse. The resolution of the apparatus combined with the transit time spread, which is a physical limitation of the cathode itself, affects the deviation of the detected temporal response from the distribution generated by the transport processes in the cathode. Some implications of these phenomena are discussed in the following.

E. Influence of time resolution on longitudinal halo study

The time resolution depends on the mode of operation. In our present measurements, the time scale for sampling the signal is set by the signal to noise ratio of the detection system, in particular, at the low intensities which are of interest in our studies. Whereas a "pulse width" measurement with the YAG screen can be obtained by sampling over less than a millisecond,[7] the present measurements require integration times of several seconds. The longer measuring time, in turn, increases the contribution of timing jitter. In addition, one has to take into account the average over time scales which are larger than the period of the magnetic stray fields which deflect the beam periodically. These fields are mainly associated with the 50 Hz frequency of the power line. Due to the defective insulator, the initial high-energy beam could not be achieved, which resulted in magnetic fluctuations larger than before. It is, therefore, not surprising that the FWHM-time resolution has worsened from about 2 ps in the best case with K_2CsSb cathode[21] conducted at 100 keV to about 5.1 ps presently (RMS values 0.9 and 2.16 ps, respectively). The RMS values can be estimated from the Gaussian-like left shoulders of the measurements presented in Fig. 6. Since the main fraction of the time response for the SSL and the K_2CsSb cathode presented in Fig. 6 is most likely contained in time intervals which are considerably

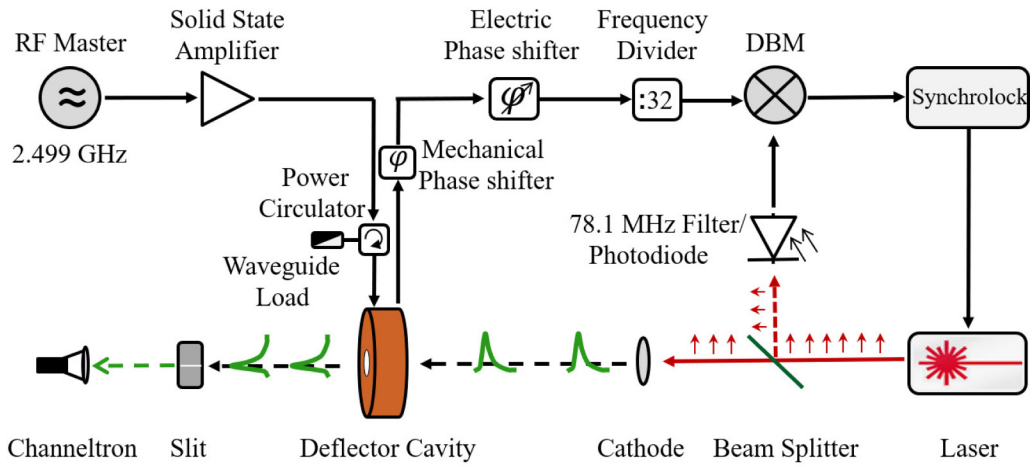

FIG. 3. Schematic overview of the principle of time response measurements. A laser pulse synchronized with the RF of the cavity generates electron pulses. As electron pulses go through the deflector cavity, the longitudinal profile of the electron bunch is transferred into a transverse profile. The transverse profile can then be detected and analyzed either by slit and channeltron method: the profile of the electron pulse is scanned through a slit, current is amplified in a channeltron, and measured with a picoammeter or alternately and by the screen method: profile of electron pulse is captured on a YAG screen and analyzed with a camera. For simplicity, the latter method is not shown in the figure.

smaller than the resolution, we can only gain limited information on the details of the response. In particular, only an upper limit for the pulse width can be obtained.

The time resolution is also affected by energy variations. It may be noted that the beam from a NEA cathode is not strictly mono-energetic but has an intrinsic energy width in the order of 0.1 eV. In addition, there exists the fluctuation and drift of the HV power supply adding to ≈1 eV.

These variations result in the following phenomenon. First, transit time spread during acceleration at the photocathode initiating from the intrinsic spread. Second, different travel times from anode to slit, due to the time varying velocities, mainly resulting from the variations of the power supply. Third, longitudinal focusing in the deflecting alpha magnet. Whereas the first two phenomena lead to an earlier arrival of particles with higher initial kinetic energy at the deflector cavity, the latter phenomenon leads to a delay for the high energetic particles since their path is longer in the alpha magnet. However, applying realistic values for the energy spreads and shifting of the voltage of the power supply, it is found that the contribution of these variations is less than a picosecond and, therefore, can be disregarded for the present investigations.

The question of longitudinal halo can nevertheless be addressed efficiently if the acceptance of the accelerator is much larger than the resolution. This is the case for most systems and, in particular, for the MESA accelerator, where the acceptance is of the order of 200 ps or more. Therefore, worsening of the resolution has insignificant influence on the specific results discussed here.

III. RESULTS

A. Quantum efficiency studies

Photocathodes with enhanced QE are desirable for accelerator operations since they require less drive-laser power to produce the same amount of current during operation. PKAT test laboratory is equipped with a tunable wavelength light source. The dependency of the QE and Mott detectors count rates asymmetry on the laser excitation wavelength was investigated and the results are presented in Fig. 4. The measured asymmetry is proportional to the polarization of the transmitted beam through the slit. For this purpose, the central wavelength was changed in the range from 768 to 871 nm, corresponding to laser energies between 1.61 and 1.42 eV, respectively.

The results indicate a strong dependency of QE on the laser energy. The quantum yield increases with energy (decreasing wavelength) to an optimum value and then remains almost constant. As the wavelength increases, the QE decreases, ranging from 0.98% to 5.02×10^{-4}%. An approximate value of the band edge energy is given by the maximum slope of the QE curve (≈800 nm).

In our investigation, the QE spectrum extends only up to 768 nm, which is equivalent to energy of 1.61 eV. Up to this energy level, our QE curve includes the first step at energy of 1.60 eV, associated with the Hh (heavy hole). Due to the limited tunability of the PKAT laser system, the second step at 1.67 eV ($\lambda \approx 740$ nm)[17] was not observable. The valance band energy splitting of the strained GaAs/GaAsP superlattice is estimated approximately 70 meV.[20]

These results are in agreement with the findings of other literature with the same strained superlattice structure.[17,22] The laser wavelength of 770.5 nm yielded the maximum QE of 0.98%. Figure 4

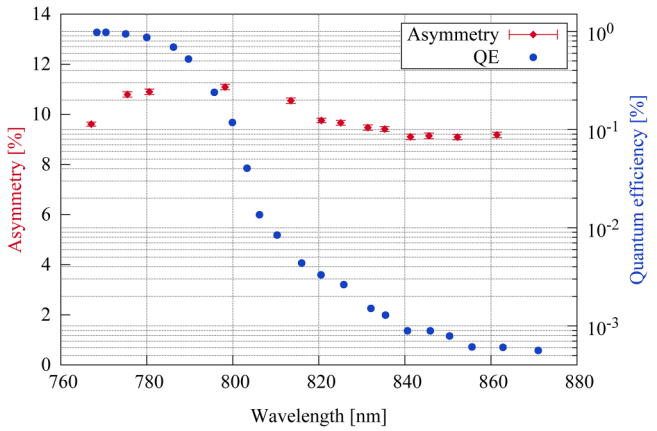

FIG. 4. Mott scattering asymmetry and quantum efficiency as a function of the exciting wavelength for the strained GaAs/GaAsP superlattice.

indicates that the accelerator operation point, where it delivers the best quality factor is at 780 ± 10 nm. A significant reduction of polarization is typically not accepted by the experimentalists. Therefore, one cannot make use of the moderate further increase of the QE at photons wavelengths shorter than 780 nm. However, at 780 nm, a QE of ≈0.9% is achieved, which for the given wavelength is a photosensitivity of greater than 5 mA/W. This QE provides sufficient conditions for operation even at future high-power linear accelerators which require intensities of several milliampere. Lasers with suitable parameters, in particular, pulse length and average power exceeding 1 W at 780 nm are commercially available.

At energies lower than the band edge, the electrons will be emitted both from the valence band and the intermediate states in the forbidden zone. Under this circumstance, thermal excitations can bridge the gap which allows photoemission in spite of the fact that the initial photon energy is insufficient. For practical purposes, excitation of a photocathode at wavelengths above the band edge is not desirable due to the low QE, as it is seen in Fig. 4.

Operating laser in the pulsed mode results in the increasing of the laser bandwidth to ≈15 nm due to the Fourier limit (time bandwidth product). The data points shown in Fig. 4 are obtained with the pulsed laser beam and, therefore, represent an averaging over this bandwidth.

B. Pulse response studies

The electron pulses from the SSL were generated with laser pulses whose central wavelength was 800 nm and with a QE of 6.41×10^{-2}%. The lifetime of the cathode used in this project is short, in the order of approximately one day. The pulse response studies were performed a few days after the activation, at a time when the QE had dropped. The measurements were conducted with the transverse deflector cavity operating at the TM_{110} mode and at the maximum input power of 322 W. This power is coupled into the cavity, and it is derived from the difference between the input and the reflected RF power.[11] Operating at the highest

possible power improves the time resolution since the deflection amplitude is proportional to $\sqrt{P}$.

In our study, to ensure precise measurement of the pulse response prior to each measurement, precautions were taken. These include, first, making sure the beam is passing through the zero crossing of the cavity, where the electric field of the cavity has minimal effect on the beam, which would otherwise accelerate or decelerate the beam. The magnetic field changes during the passing of the electron pulse through the cavity. However, the entrance phase can be adjusted so that the electrons reach the center of the cavity when the field is zero. Second and of equal importance, ascertaining that the beam is well focused with the smallest transverse diameter at the slit position to allow high resolution measurements. Third, avoiding excessive space charge defocusing is essential. According to the previous investigations in the PKAT system,[5] it was estimated that a typical bunch charge should be limited to the maximum 0.1 fC. This charge is equivalent to approximately 620 electrons per bunch. For operation at 78.1 MHz, that amount translates to currents of $I < 10$ nA. Therefore, to avoid space charge defocusing and to prevent damaging the channeltron by excess current, an average beam current of 1–3 nA was chosen throughout our measurements. A typical contribution of the absolute dark base current level for the channeltron is in the order of 10^{-15} A, which corresponds to 10^{-4} of the signal, and it has been accounted for by subtracting it.

Using the diameter of the YAG screen as the scale, the screen can be calibrated, $1\ \text{px} = (52.3 \pm 0.2)\ \mu\text{m}$. Next, the conversion relationship of $5.67\ \text{ps mm}^{-1}$ at maximum power of the deflector cavity is obtained. These two equations provide the necessary information for the screen calibration in terms of the phase shift. A typical transverse beam size at the location of the YAG screen was measured with σ of about $140\ \mu\text{m}$, which corresponds to 0.79 ps in temporal profile,[20] see Fig. 5. The transverse beam width, therefore, contributes to time resolution although to a lesser amount than the effect of the aforementioned synchronization jitter. The result of temporal response of the SVT GaAs/GaAsP superlattice photocathode along with the transverse beam diameter is shown in Fig. 5.

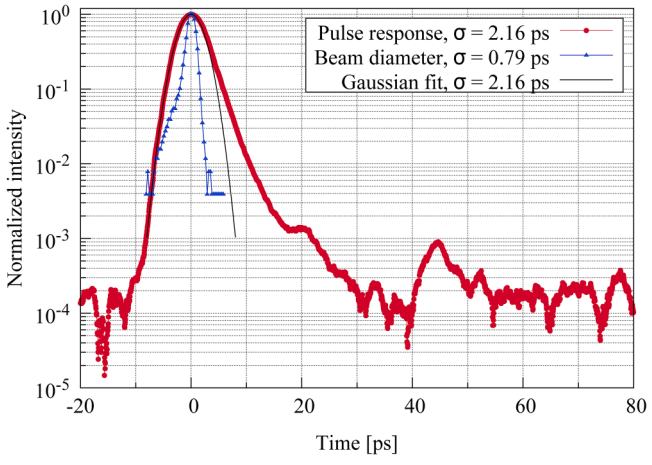

FIG. 5. Temporal response of a strained GaAs/GaAsP superlattice photocathode. The blue curve represents the transverse beam diameter at the location of the slit. In order to illustrate the behavior of the data, a Gaussian curve with $\sigma = 2.16$ ps, shown in black, is added to Fig. 5. The pulse response is almost Gaussian for approximately 2σ and then it deviates from the Gaussian curve.

The superlattice pulse response around the peak intensity is almost Gaussian for approximately $\pm 2\,\sigma_{\text{RMS}}$, where $\sigma_{\text{RMS}} = 2.16$ ps is obtained from the Gaussian fit. For the left shoulder, assuming that the electron emission should start immediately after excitation, and if ideally all of the electrons have the same energy at the surface, one expects an infinitely steep curve on the left. However, due to the time resolution of the apparatus and the transit time spread caused by the initial energy distribution, there will be a non-zero rise time. Since the calculations of the resulting transit time spread are well below the observed time constant, it can be inferred that the rising edge is dominated by the experimental resolution for which the $\sigma_{\text{RMS}} = 2.16$ ps can be set as an upper limit.

The right shoulder of the peak is influenced by the transport processes of the cathode. A slight elongation with respect to the left shoulder and a somewhat different curvature is observed. This observation indicates an approximately exponential behavior during the time interval between 5 and 15 ps. There exist several possibilities in explaining this behavior. For instance, thermal emission from the bound states is located near the photoemission threshold in the surface region. This assumption is in approximate agreement with the results for the dynamics of electron density in the surface states of GaAs samples grown with the gradient doped MBE. These were recently measured using a pump probe technique by Zhou *et al.*,[23] in which a fast decay of surface electron density with a time constant of 1.5 ps was observed.

In view of practical implications, it can be stated that we have observed an upper limit of $\sigma_{\text{RMS}} = 2.16$ ps for the RMS width of the response, and for times greater than 5 ps, an exponential contribution with a time constant of $\approx$2.4 ps. As previously mentioned, since the typical acceptance of accelerators can be an order of magnitude larger, the time response of the SSL is compatible with low loss requirements. However, as shown in Fig. 5, the exponential decay stops after approximately 15 ps.

The small humps in the low intensity region typically have a similar shape compared to the main pulse. It seems unlikely that they are the result of a transport phenomenon of the semiconductor. The observed fluctuations after the main pulse may be the result of the double reflection of the laser from the optics on the path of the laser. After the laser beam is produced, it travels through several optical elements (such as polarizer, telescope, and window) before reaching the photocathode. As the laser beam passes through the interface of two media with different refractive indices, a fraction of the incident laser intensity is reflected. These reflected intensities will create parasite pulses which illuminate the cathode at different times than the main laser pulse. The arrival times are given by 2d/c, where d is the distance between the two surfaces and c is the speed of light. The distance between window and cathode is $\approx$100 cm, while the distance between the two sides of the polarizer is approximately 1 cm.

The phase shift induced by the different distances of the surfaces is depending of the arrangement of the optical elements. Whereas the two surfaces of the entrance window cause a delay of

the double reflected pulse of a few picoseconds only, the one caused by the double reflection from the cathode surface and the entrance window amount to several RF periods. The distances between the surfaces are vastly different resulting in additional fractional residuals of arrival times in units of the radio frequency period. As a result, the additional peaks can happen at any position in phase. It is, therefore, not surprising that the humps in the intensity occur at seemingly random positions.

Averaged over the time period from 30 to 80 ps, the longitudinal halo of GaAs/GaAsP superlattice is of the order of 3.0×10^{-4} compared to the peak intensity. Comparing our results with the previous results from AlInGaAs/AlGaAs SSL photocathode performed with electron beam energy of 100 keV[8] indicates that the longitudinal halo of strained GaAs/GaAsP superlattice is at least by two orders of magnitude smaller than the halo in those measurements. This proves the better quality performance of the SVT superlattice in obtaining short pulses.

Figure 6 illustrates the comparison of the impulse response measurements between the strained GaAs/GaAsP superlattice, K_2CsSb, and a typical bulk GaAs photocathode, taken at QE of 6.1×10^{-2}%, 1%, and 5.8%, respectively.

K_2CsSb cathodes belong to the positive electron affinity (PEA) group, and as such, the vacuum level is above the conduction band minimum. In a PEA cathode, only the electrons which have an energy above the vacuum level after transporting to the surface can be emitted into the vacuum. The PEA photocathodes offer lower electron energy spread and, thus, provide high-brightness beams and lower longitudinal halo. The investigations of K_2CsSb were conducted at 400 nm excitation wavelength and with a 100 keV energy electron beam.[24] Furthermore, less noisy electronics were used during the investigations and lower noise condition was achieved.

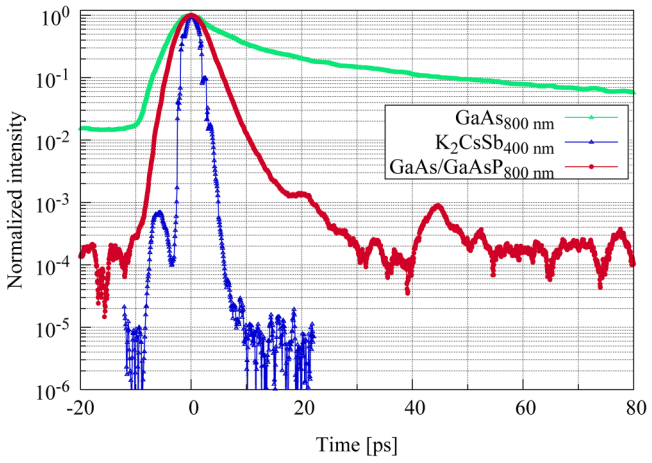

FIG. 6. The comparison of temporal response measurements of strained GaAs/GaAsP superlattice with K_2CsSb and bulk GaAs photocathodes. The pulse responses of GaAs/GaAsP and bulk GaAs are obtained at a beam energy of 45 keV and an excitation wavelength of 800 nm, whereas K_2CsSb is measured with a 100 keV beam and at 400 nm excitation.

GaAs/GaAsP SSL has a longitudinal halo more than 2.5 orders of magnitude smaller than bulk GaAs. This difference clearly illustrates the improvement that one achieves using strained GaAs/GaAsP superlattice rather than the bulk in producing short pulses. In bulk, the active layer is the entire thickness of crystal (510–517 μm). However, for general purposes, it is sufficient to take into account only a few diffusion lengths (in the order of μm) in which the majority of the photoexcited electrons are generated. However, the superlattice has an active layer thickness of ≈92 nm. The electrons are generated close to the surface and can be emitted much faster into the vacuum.

K_2CsSb has a faster response and a longitudinal halo at a level of about 6×10^{-5} compared to the intensity maximum. This suggests an advantage of the PEA K_2CsSb cathodes over the NEA cathodes for high-brightness electron beam applications. This advantage results from the PEA state of the cathode. In a PEA cathode, the thermalization process leads to reduction of the electrons which can overcome the photoemission threshold since by definition the lower conduction band states have an energy below the vacuum level in PEA cathodes. This process happens on the picosecond time scale. This is in stark contrast to the NEA situation, where electrons can escape whenever they reach the surface and are depleted only (besides emission into vacuum and trapping in the surface region) by the carrier lifetime in the conduction band. In the case of the NEA cathodes, the carrier lifetime is of the order 100 ps or longer.

In order to overcome the work function, the K_2CsSb response measurement was conducted at 400 nm. In addition, the experiment with K_2CsSb has been conducted at 100 keV compared to the 45 keV for the SSL GaAs/GaAsP, which resulted in a better time resolution for the K_2CsSb measurement. Moreover, in the investigation with K_2CsSb, other pulses with higher longitudinal halo in the order of 2×10^{-4} have been observed.[21] For an equitable comparison, one must compare the pulse response of the strained GaAs/GaAsP superlattice at 400 nm and with a beam energy of 100 keV.

In the K_2CsSb investigations, it is speculated that the hump on the rising edge is possibly due to the double reflection of the laser from the optics on the path of the laser. More investigation is required to specify the reason for the observed hump. The pulse response of GaAs/GaAsP shows a slight change of slope in the same region. However, due to the better time resolution in the K_2CsSb measurements (at least by a factor of two), the hump is more apparent. The K_2CsSb measurements were conducted at 400 nm which require frequency doubling of the laser pulses. The light polarization optics (Pockels cell and polarizer) were not present during the investigations. These circumstances can lead to an effective suppression of double reflections since there exist less optical surfaces. Under these conditions, parasitic pulses, which may come from the laser itself, are suppressed by the frequency doubling due to the quadratic dependence of this process on the input intensity.

The distinguishing characteristic of the strained GaAs/GaAsP superlattice compared to the K_2CsSb and the bulk GaAs is its ability to produce highly spin-polarized electrons. As previously discussed, producing beams of highly polarized electrons requires the degeneracy of valence bands to be broken. While it is not possible to generate highly spin-polarized electrons from GaAs to our

knowledge, no definitive experimental result is available for K_2CsSb. It is, however, not likely that high spin polarization can be generated from these PEA cathodes since electron states high above the conduction band minimum have to be excited which should not correspond to a quantum mechanical S-state.

IV. CONCLUSIONS

The strained GaAsP/GaAs superlattice photocathode offers a sufficiently fast response with a small longitudinal halo and a QE which makes intensities in the milliampere range feasible. These qualities in conjunction with the high degree of spin polarization make this superlattice photocathode suitable for high-power accelerators dedicated to fundamental research, such as MESA.

Optical imperfections generated a longitudinal halo of the order of 10^{-4} relative to the peak intensity in our measurements. Although such a halo may be further suppressed in a dedicated laser optical setup, it seems advisable to block the halo at low accelerator energies by using a chopper system. Therefore, using a chopper for longitudinal collimation and, hence, further reduction of the halo at high energies is suggested.

ACKNOWLEDGMENTS

The authors would like to thank Dr. Werner Lauth for the tremendous assistance in minimizing the noise problem for polarization measurements.

AUTHOR DECLARATIONS

Conflict of Interest

The authors have no conflicts to disclose.

Author Contributions

Nahid Scahill: Conceptualization (equal); Data curation (lead); Formal analysis (lead); Investigation (lead); Methodology (equal); Project administration (equal); Resources (equal); Software (lead); Validation (equal); Visualization (equal); Writing – original draft (lead); Writing – review & editing (lead). **Kurt Aulenbacher:** Conceptualization (equal); Data curation (supporting); Formal analysis (supporting); Funding acquisition (lead); Investigation (supporting); Methodology (supporting); Project administration (lead); Resources (equal); Software (supporting); Supervision (lead); Validation (equal); Visualization (equal); Writing – original draft (supporting); Writing – review & editing (supporting).

DATA AVAILABILITY

The data that support the findings of this study are available from the corresponding author upon reasonable request.

REFERENCES

[1]F. Hug, K. Aulenbacher, R. Heine, B. Ledroit, and D. Simon, "MESA—An ERL project for particle physics experiments," in *28th International Linear Accelerator Conference* (JACOW, 2017), p. MOP106012.
[2]D. Becker *et al.*, "The P2 experiment," Eur. Phys. J. A **54**, 208 (2018).
[3]K. Aulenbacher *et al.*, "The MAMI source of polarized electrons," Nucl. Instrum. Methods Phys. Res. A **391**, 498–506 (1997).
[4]D. Britzger, "The large hadron electron collider," J. Phys. G **48**, 110501 (2021).
[5]K. Aulenbacher, J. Schuler, D. Harrach, J. Röthgen, and E. Reichert, "Pulse response of thin III/V semiconductor photocathodes," J. Appl. Phys. **92**, 7536 (2002).
[6]K. Aulenbacher, "Erzeugung hochpolarisierter Elektronenstrahlen mit hoher Symmetrie unter Helizitätswechsel Habilitation," Habilitation Thesis (Johannes Gutenberg-Universität Mainz, 2007).
[7]E. Riehn, "Photokathoden mit internem DBR-Reflektor als Quellen hochintensiver spinpolar-isierter Elektronenstrahlen," Ph.D. thesis (University of Mainz, 2011).
[8]L. G. Gerchikov, K. Aulenbacher, Y. A. Mamaev, E. J. Riehn, and Y. P. Yashin, "Transport and partial localization of electrons in strained short-period semiconductor superlattices," Semiconductors **46**, 67–74 (2012).
[9]W. E. Spicer and A. Herrera-Gomez, "Modern theory and applications of photocathodes," in *Photodetectors and Power Meters* (International Society for Optics and Photonics, 1993), Vol. 2022, pp. 18–35.
[10]L. Cultrera, J. Maxson, I. Bazarov, S. Belomestnykh, J. Dobbins, B. Dunham, S. Karkare, R. Kaplan, V. Kostroun, Y. Li *et al.*, "Photocathode behavior during high current running in the Cornell energy recovery linac photoinjector," Phys. Rev. Spec. Top. Accel. Beams **14**, 120101 (2011).
[11]P. Hartmann, J. Bermuth, J. Hoffmann, S. Köbis, E. Reichert, H. Andresen, K. Aulenbacher, P. Drescher, H. Euteneuer, H. Fischer *et al.*, "Picosecond polarized electron bunches from a strained layer GaAsP photocathode," Nucl. Instrum. Methods Phys. Res. A **379**, 15–20 (1996).
[12]C. K. Sinclair, P. A. Adderley, B. M. Dunham, J. C. Hansknecht, P. Hartmann, M. Poelker, J. S. Price, P. M. Rutt, W. J. Schneider, and M. Steigerwald, "Development of a high average current polarized electron source with long cathode operational lifetime," Phys. Rev. Spec. Top. Accel. Beams **10**, 023501 (2007).
[13]D. A. Orlov, C. Krantz, A. Wolf, A. S. Jaroshevich, S. N. Kosolobov, H. E. Scheibler, and A. S. Terekhov, "Long term operation of high quantum efficiency GaAs (Cs, O) photocathodes using multiple recleaning by atomic hydrogen," J. Appl. Phys. **106**, 054907 (2009).
[14]S. Karkare, D. Dimitrov, W. Schaff, L. Cultrera, A. Bartnik, X. Liu, E. Sawyer, T. Esposito, and I. Bazarov, "Monte Carlo charge transport and photoemission from negative electron affinity GaAs photocathodes," J. Appl. Phys. **113**, 104904 (2013).
[15]K. Aulenbacher, I. Alexander, E. Riehn, and V. Tioukine, "High average photocurrent research at MAMI," J. Phys. Conf. Ser. **298**, 012019 (2011).
[16]K. Aulenbacher, "Polarized beams for electron accelerators," Eur. Phys. J. Spec. Top. **198**, 361–380 (2011).
[17]T. Maruyama, D.-A. Luh, A. Brachmann, J. E. Clendenin, E. Garwin, S. Harvey, J. Jiang, R. E. Kirby, C. Y. Prescott, R. Prepost, and A. M. Moy, "Systematic study of polarized electron emission from strained GaAs/GaAsP superlattice photocathodes," Appl. Phys. Lett. **85**, 2640–2642 (2004).
[18]See https:www.svta.com for "SVT Associates, Inc., Eden Prairie, MN, USA."
[19]D. T. Pierce and F. Meier, "Photoemission of spin-polarized electrons from GaAs," Phys. Rev. B **13**, 5484 (1976).
[20]N. Scahill, "Self-modulation of photoemitted bunches at the picosecond timescale," Ph.D. thesis (Johannes Gutenberg-Universität Mainz, 2022).
[21]V. Bechthold, "Investigation of multi-alkali compounds with regard to their suitability for generating high-brilliance electron pulses," Ph.D. thesis (Universityätsbibliothek Mainz, 2019).
[22]W. Liu, Y. Chen, W. Lu, A. Moy, M. Poelker, M. Stutzman, and S. Zhang, "Record-level quantum efficiency from a high polarization strained GaAs/GaAsP superlattice photocathode with distributed Bragg reflector," Appl. Phys. Lett. **109**, 252104 (2016).
[23]R. Zhou, H. Jani, Y. Zhang, Y. Qian, and L. Duan, "Photoelectron transportation dynamics in GaAs photocathodes," J. Appl. Phys. **130**, 113101 (2021).
[24]V. Bechthold, K. Aulenbacher, M. Dehn, S. Friederich *et al.*, "Investigation of K_2CsSb photocathodes," in *Proceedings of the 59th ICFA Advanced Beam Dynamics Workshop on Energy Recovery Linacs, Geneva, Switzerland* (JACOW, 2017), pp. 4–8.